

A Simple Lifelong Learning Approach

Joshua T. Vogelstein,^{1,†} Jayanta Dey,^{1,†,*} Hayden S. Helm,¹ Will LeVine,¹ Ronak D. Mehta,¹ Tyler M. Tomita,¹ Haoyin Xu,¹ Ali Geisa,¹ Qingyang Wang,¹ Guido M. van de Ven,^{2,3} Chenyu Gao,¹ Weiwei Yang,⁴ Bryan Tower,⁴ Jonathan Larson,⁴ Christopher M. White,⁴ and Carey E. Priebe¹

Abstract. In lifelong learning, data are used to improve performance not only on the present task, but also on past and future (unencountered) tasks. While typical transfer learning algorithms can improve performance on future tasks, their performance on prior tasks degrades upon learning new tasks (called forgetting). Many recent approaches for continual or lifelong learning have attempted to *maintain* performance on old tasks given new tasks. But striving to avoid forgetting sets the goal unnecessarily low. The goal of lifelong learning should be to use data to improve performance on both future tasks (forward transfer) and past tasks (backward transfer). In this paper, we show that a simple approach—representation ensembling—demonstrates both forward and backward transfer in a variety of simulated and benchmark data scenarios, including tabular, vision (CIFAR-100, 5-dataset, Split Mini-Imagenet, and Food1k), and speech (spoken digit), in contrast to various reference algorithms, which typically failed to transfer either forward or backward, or both. Moreover, our proposed approach can flexibly operate with or without a computational budget.

1 Introduction Learning is a process by which an intelligent system improves performance on a given task by leveraging data [1]. In classical machine learning, the system is often optimized for a single task [2, 3]. While it is relatively easy to *simultaneously* optimize for multiple tasks (multi-task learning) [4], it has proven much more difficult to *sequentially* optimize for multiple tasks [5, 6]. Specifically, classical machine learning systems, and natural extensions thereof, exhibit “catastrophic forgetting” when trained sequentially, meaning their performance on the prior tasks drops precipitously upon training on new tasks [7, 8]. However, learning could be lifelong, with agents continually building on past knowledge and experiences, improving on many tasks given data associated with any task. For example, in humans, learning a second language often improves performance in an individual’s native language [9].

In the past 30 years, a number of sequential task learning algorithms have attempted to overcome catastrophic forgetting. These approaches naturally fall into one of two camps. In one camp, the algorithm has fixed resources, and so must reallocate resources (essentially compressing representations) in order to incorporate new knowledge [10–14]. Biologically, this corresponds to adulthood, where brains have a nearly fixed or decreasing number of cells and synapses. In the other camp, the algorithm adds (or builds) resources as new data arrive (essentially ensembling representations) [15–18]. Biologically, this corresponds to development, where brains grow by adding cells, synapses, etc.

Approaches from both camps demonstrate some degree of continual (or lifelong) learning [19]. In particular, they can sometimes learn new tasks faster due to prior learning on related tasks, while not catastrophically forgetting old tasks (see Appendix .1 for a detailed discussion on the relevant algorithms). However, as we will show, many lifelong learning algorithms are unable to transfer knowledge forward (to future unseen tasks) and most of them do not transfer backward (to previously seen tasks). With high enough sample sizes, some of these algorithms are able to transfer forward or backward, but transfer is more important in low sample size regimes [17, 20]. This inability to effectively transfer in low-sample size regimes has been identified as one of the key obstacles limiting the capabilities of artificial intelligence [21, 22].

In this paper, we propose a general approach for lifelong learning which can be used with many existing encoder models. Specifically, we focus our approach on ensembling deep networks (Sim-

¹Johns Hopkins University, ²Baylor College of Medicine, ³University of Cambridge, ⁴Microsoft Research,

[†]denotes equal contribution, ^{*}corresponding author: jdey4@jhu.edu

ple Lifelong Learning Networks, SiLLY-N). Additionally, we demonstrate how the same approach can be generalized for lifelong learning based on ensembling decision forests (Simple Lifelong Learning Forests, SiLLY-F). We explore our proposed algorithm as compared to a number of reference algorithms on an extensive suite of numerical experiments that span simulation, vision datasets including CIFAR-100, 5-dataset, Split Mini-Imagenet, and Food1k, as well as the spoken digit dataset. Figure 1 illustrates that our algorithm outperforms all the reference algorithms in terms of forward, backward, and overall transfer on CIFAR 10X10 dataset. Ablation studies indicate the degree to which the amount of representation or storage capacity and replaying old task data impact performance of our algorithms. All our code and experiments are open source to facilitate reproducibility.

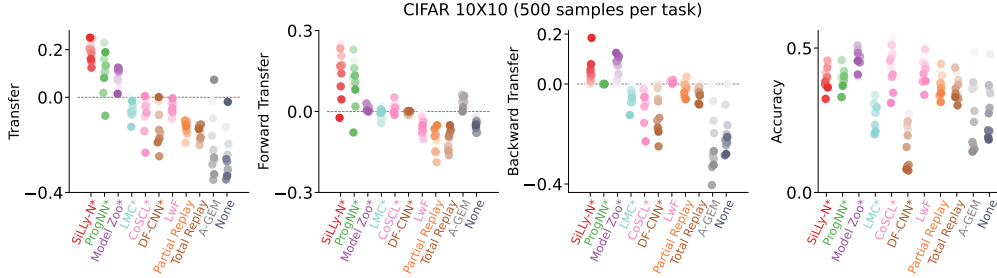


Figure 1: **Performance summary on CIFAR 10X10 benchmark dataset.** Columns are different evaluation criteria (see Section 2 for definitions, and Section 6 for experimental details), each strip of colored dots corresponds to an algorithm (we introduce SiLLY-N here) and each dot represents a task. In all the figure, older tasks have darker colors. Resource growing algorithms have a '*'. EWC, O-EWC, SI, TAG and ER always perform worse than LwF, and hence we do not show them in the plot. SiLLY-N (red) outperforms all reference algorithms in terms of forward (second panel), backward (third panel), and overall transfer (first panel). Importantly, such better transfer is achieved at high overall accuracy (last panel). More datasets are evaluated in Figure 8.

2 Mathematical Framework

2.1 The lifelong learning objective Consider a lifelong or continual learning environment with tasks, $\mathcal{T} = \{1, 2, \dots, T\}$. We consider task aware lifelong learning, i.e., the tasks are known during both training and testing time. For simplicity, we consider that any task $t \in \mathcal{T}$ has the same input space, i.e., they have $\mathcal{X} \subset \mathbb{R}^D$ valued inputs with $\mathcal{Y} = \{1, \dots, K_t\}$ valued class labels. We assume the tasks arrive sequentially, but the n_t data samples within each task t , $\mathbf{S}^t = \{(X_i, Y_i)\}_{i=1}^{n_t}$, are batched and sampled identically and independently (*iid*) from some fixed distribution \mathcal{D}_t , and $\sum_{t=1}^T n_t = n$. A learner $f \in \mathcal{F}$ trains on \mathbf{S}^t and chooses a hypothesis $h_t \in \mathcal{H}$ associated with task t by minimizing a particular risk, where \mathcal{F} and \mathcal{H} are the algorithm and the hypothesis space, respectively. In supervised learning settings, one can consider the following risk for a particular task t :

$$(1) \quad R^t(f(\mathbf{S}^t)) = R^t(h_t) = \mathbb{E}_{(X,Y) \sim \mathcal{D}_t}[\ell_t(h_t(X), Y)],$$

where $\ell_t : \mathcal{Y} \times \mathcal{Y} \rightarrow [0, \infty)$ is a given loss function associated with the task t and $h_t = f(\mathbf{S}^t)$. Note that the data \mathbf{S}^t may contain data that is relevant to any number of tasks (potentially all the tasks) in the environment. One may take expectation over \mathbf{S}^t and consider the generalization error for the task as:

$$(2) \quad \mathcal{E}_f^t(\mathbf{S}^t) = \mathbb{E}[R^t(f(\mathbf{S}^t))].$$

In the above equation, the learner will have access to a total of T datasets after T tasks, $\bigcup_{t=1}^T \mathbf{S}^t$, instead of \mathbf{S}^t only¹. The goal is to find a learner $f \in \mathcal{F}$ that chooses a set of total T hypotheses

¹More generally, we may have J datasets, where $J \neq T$ and each dataset may be associated with the target distributions of multiple tasks. For simplicity, we do not consider such scenarios further at this time.

$\{h_1, \dots, h_T\}$ (one hypothesis for each task) such that the generalization error over all the tasks after observing all the data is minimized, that is:

$$(3) \quad \begin{array}{ll} \text{minimize} & \sum_{t=1}^T \mathcal{E}_f^t(\mathbf{U}_{t'=1}^T \mathbf{S}^{t'}) \\ \text{subject to} & f \in \mathcal{F} \end{array} .$$

2.2 Lifelong learning evaluation criteria Others have previously introduced criteria to evaluate transfer, including forward and backward transfer [23–26]. Pearl [27] introduced the transfer benefit ratio, which builds directly off relative efficiency from classical statistics [28]. We define three notions of transfer building on relative efficiency.

Definition 1 (Transfer). *Overall transfer of algorithm f for a given Task t is:*

$$(4) \quad \text{Transfer}^t(f) := \log \frac{\mathcal{E}_f^t(\mathbf{S}^t)}{\mathcal{E}_f^t(\mathbf{U}_{t'=1}^T \mathbf{S}^{t'})} .$$

We say that an algorithm f has transferred to task t from all the tasks up to T if and only if $\text{Transfer}^t(f) > 0$.

Forward transfer quantifies how much performance a learner transfers forward to future tasks, given prior tasks.

Definition 2 (Forward Transfer). *The forward transfer of f for task t is :*

$$(5) \quad \text{Forward Transfer}^t(f) := \log \frac{\mathcal{E}_f^t(\mathbf{S}^t)}{\mathcal{E}_f^t(\mathbf{U}_{t'=1}^t \mathbf{S}^{t'})} .$$

We say an algorithm (positively) forward transfers for task t if and only if:

$$(6) \quad \text{Forward Transfer}^t(f) > 0 .$$

Backward transfer quantifies how much a learner transfers backward to previously observed tasks, in light of new tasks.

Definition 3 (Backward Transfer). *The backward transfer of f for Task t is:*

$$(7) \quad \text{Backward Transfer}^t(f) := \log \frac{\mathcal{E}_f^t(\mathbf{U}_{t'=1}^t \mathbf{S}^{t'})}{\mathcal{E}_f^t(\mathbf{U}_{t'=1}^T \mathbf{S}^{t'})} .$$

We say an algorithm backward transfers to Task t from all the future tasks up to T if and only if:

$$(8) \quad \text{Backward Transfer}^t(f) > 0 .$$

Note that Transfer can be decomposed into Forward Transfer and Backward Transfer:

$$(9) \quad \text{Transfer}^t(f) = \log \frac{\mathcal{E}_f^t(\mathbf{S}^t)}{\mathcal{E}_f^t(\mathbf{U}_{t'=1}^T \mathbf{S}^{t'})}$$

$$(10) \quad = \log \frac{\mathcal{E}_f^t(\mathbf{S}^t)}{\mathcal{E}_f^t(\mathbf{U}_{t'=1}^t \mathbf{S}^{t'})} + \log \frac{\mathcal{E}_f^t(\mathbf{U}_{t'=1}^t \mathbf{S}^{t'})}{\mathcal{E}_f^t(\mathbf{U}_{t'=1}^T \mathbf{S}^{t'})}$$

$$(11) \quad = \text{Forward Transfer}^t(f) + \text{Backward Transfer}^t(f) .$$

Another paper [26], concomitantly introduced transfer and forgetting (backward transfer). Their statistics are the same as ours, except they do not use a log. We opted for a log to address numerical stability issues in comparing small numbers. Because log is a monotonic function, the order of ranking algorithms is preserved (Appendix Figure 1 shows a version of Figure 1 and Figure 8, but using Veniat’s statistics, which is nearly visually identical). By virtue of introducing Forward Transfer here, we can identify the inherent trade-off between forward and backward transfer, for a fixed amount of total transfer. Apart from the above statistics, we also report accuracy per task.

Definition 4 (Accuracy). *The accuracy of algorithm f on task t after observing total T datasets is:*

$$(12) \quad \text{Accuracy}^t(f) := 1 - \mathcal{E}_f^t\left(\bigcup_{t'=1}^T \mathbf{S}^{t'}\right).$$

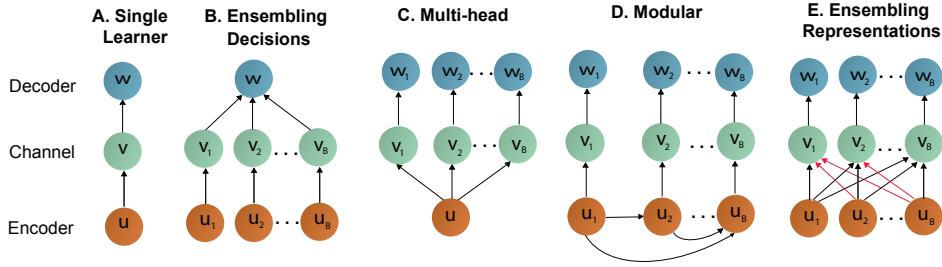


Figure 2: Schemas of composable hypotheses. A. Single task learner. B. Ensembling decisions (as output by the channels) is a well-established practice, including random forests and gradient boosted trees. C. Learning a joint representation or D. learning future representations depending on the past encoders was previously used in lifelong learning scenarios, but encoders were not trained independently as in E. Note that the new encoders in E interact with the previous encoders through the channel layer (indicated by red arrows), thereby, enabling backward transfer. Again the old encoders interact with the future encoders (indicated by black arrows), thereby, enabling forward transfer.

3 Representation ensembling algorithms Shannon proposed that a learned hypothesis can be decomposed into three components: an encoder, a channel, and a decoder [29, 30]: $h(\cdot) = w \circ v \circ u(\cdot)$. Figure 2 shows these three components as the building blocks of different learning schemas. The encoder, $u : \mathcal{X} \mapsto \tilde{\mathcal{X}}$, maps an \mathcal{X} -valued input into an internal representation space $\tilde{\mathcal{X}}$ [31, 32]. The channel $v : \tilde{\mathcal{X}} \mapsto \Delta_{\mathcal{Y}}$ maps the transformed data into a posterior distribution (or, more generally, a score). Finally, a decoder $w : \Delta_{\mathcal{Y}} \mapsto \mathcal{Y}$, produces a predicted label.

A canonical example of a single learner depicted in Figure 2A is a decision tree. Importantly, one can subsample the training data to learn different components of the tree [33–35]. For example, one can use a portion of data to learn the tree structure (which is the encoder). Then, by pushing the remaining data (sometimes called the ‘out-of-bag’ data) through the tree, one can learn posteriors in each leaf node (which are the channel). The channel thus gives scores for each data point denoting the probability of that data point belonging to a specific class. Using separate sets of data to learn the encoder and the channel results in less bias in the estimated posterior in the channels as in ‘honest trees’ [33–35]. Finally, the decoder provides the predicted class label using argmax over the posteriors from the channel.

One can generalize the above decomposition by allowing for multiple encoders, as shown in Figure 2B. Given B different encoders, one can attach a single channel to each encoder, yielding B different channels. Doing so requires generalizing the definition of a decoder so that it would operate on multiple channels. Such a decoder ensembles the *decisions*, because here each channel provides the final output based on the encoder. This is the learning paradigm behind bagging [36] and boosting [37]; indeed, decision forests are a canonical example of a decision function operating on an ensemble of B outputs [38].

Although the task specific structure in Figure 2B can provide useful decision on the corresponding task, they cannot, in general, provide meaningful decisions on other tasks, because those tasks might have completely different class labels. Therefore, in the multi-head structure (Figure 2C) a single encoder is used to learn a joint representation from all the tasks, and a separate channel is learned for each task to get the score or class conditional posteriors for each task, which is followed by each task specific decider [10, 11, 13].

Modular approaches, such as PROGN and LMC (Figure 2D), have both multiple encoders and decoders. Connections from past to future encoders enables forward transfer. However, they freeze backward transfer.

Our approach also uses multiple encoders and decoders (Figure 2E). Unlike modular approaches, we allow interaction among encoders through the channels, including both forward and backward interactions. The result is that the channels **ensemble representations** (learned by the encoders), rather than decisions (learned by the channels as in Figure 2 B). In our algorithms, we push all the data through each encoder, and each channel learns and ensembles across all encoders. When each encoder has learned complementary representations, the channels can leverage that information to improve over single task performance. This approach has applications in few-shot and multiple task scenarios, as well as lifelong learning.

3.1 Our representation ensembling algorithms Figure 2E shows a general structure of our algorithm. As data from a new task arrives, the algorithm first builds a new encoder. Then, it builds the channel for this new task by pushing the new task data through *all* existing encoders. Thus the channel integrates information across all existing encoders using the new task data, thereby enabling forward transfer. At the same time, if it stores old task data (or can generate such data), it can push that data through the new encoders to update the channels from the old tasks, thereby enabling backward transfer. In either case, new test data are passed through all existing encoders and corresponding channels to make a prediction (see appendix for detailed description of this approach).

Simple Lifelong Learning Networks in resource growing mode A Simple Lifelong Learning Network (SILLY-N) ensembles deep networks. For each task, the encoder u_t in SILLY-N is the “backbone” of a deep network (DN). Thus, each u_t maps an element of \mathcal{X} to an element of \mathbb{R}^d , where d is the number of neurons in the penultimate layer of the DN. The channels are learned by averaging over k -Nearest Neighbors (k -NN) [39] trained over the d dimensional representations of \mathcal{X} . Note that the channel is trained on the d dimensional outputs from the encoders which is much smaller in size than the original training data and hence, the k -NN channels are inexpensive storage-wise (shown later in Figure 3). Other algorithms could also be used to learn the channels, though we do not pursue them here. The decoder w_t outputs the argmax to produce a single prediction.

Simple Lifelong Learning Networks in resource constrained mode The above resource growing approach is ideal when the upcoming tasks become more and more complex and there is no constraint imposed by the computation and storage budget available. However, real-world scenarios often impose computational constraints. In the constant resource mode, we stop building new encoders after we have reached the computation and the storage budget imposed by the user. As new tasks arrive, we only learn new channels associated with new tasks using the old encoders. Note that this approach completely excludes the need to save old task data after we have reached the budget.

Hereafter, we will use suffix ‘-M’ after the algorithm name whenever we use resource constrained operation of SILLY-N. Here M is the total number of encoder allowed by the budget.

Additional realization of our approach using random forest as encoder Simple Lifelong Learning Forest (SILLY-F) ensembles decision trees or forests. For each task, the encoder u_t of SILLY-F is the representation learned by a decision forest [38, 40]. The channel then learns the class-conditional posteriors by populating the forest leaves with out-of-task samples, as in “honest trees” [33–35]. Each

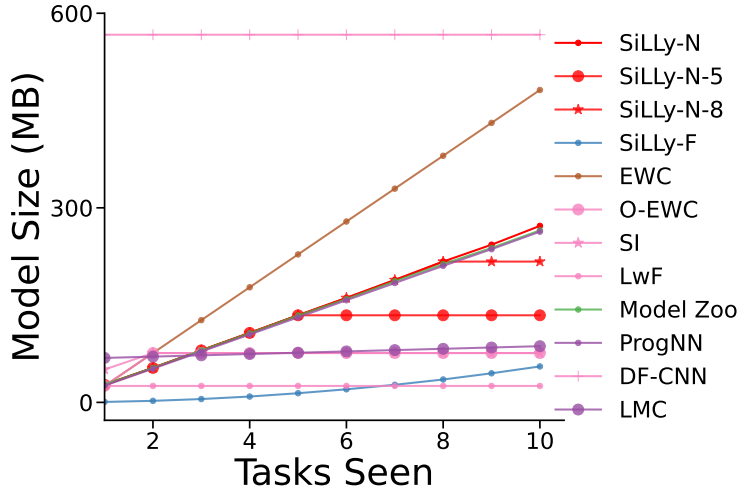


Figure 3: **Storage space as a function on number of tasks in CIFAR 10X10.** Memory consumed by SiLLy-N is dominated by the encoder size. The size of DF-CNN remains constant throughout.

channel outputs the posteriors averaged across the collection of forests learned over different tasks. The decoder w_t outputs the argmax to produce a single prediction.

Note that the amount of additional representation capacity added per task by SiLLy-F is a function of the amount and complexity of the data for a new task. Contrast this with SiLLy-N and other deep net based modular or representation ensembling approaches, which *a priori* choose how much additional representation to add, prior to seeing all the new task data. So, SiLLy-F has capacity, space complexity, and time complexity scale with the complexity and sample size of each task. In contrast, ProgNN, SiLLy-N (and others like it) have a fixed capacity for each task, even if the tasks have very different sample sizes and complexities.

4 A computational taxonomy of lifelong learners The space complexity of the learner refers to the amount of memory space needed to store the learner [41]. We also study the representation capacity of these algorithms. Capacity is defined as the size of the subset of hypotheses that is achievable by the learning algorithm [42].

We use the soft-O notation \tilde{O} to quantify complexity [43]. Letting n be the sample size and T be the number of tasks, we write that the capacity, space or time complexity of a lifelong learning algorithm is $f(n, t) = \tilde{O}(g(n, T))$ when $|f|$ is bounded above asymptotically by a function g of n and T up to a constant factor and polylogarithmic terms. For simplifying the calculation, we make the following assumptions:

1. Each task has the same number of training samples.
2. Capacity grows linearly with the number of trainable parameters in the model.
3. The number of epochs is fixed for each task.
4. For the algorithms with dynamically expanding capacity, we assume the worst case scenario where an equal amount of capacity is added to the hypothesis with an additional task.

Assumption 3 enables us to write time complexity as a function of the sample size. Table 1 summarizes the capacity, space and time complexity of several reference algorithms, as well as our SiLLy-N and SiLLy-F. For space and time complexity, the table shows results as a function of n and T , as well as the common scenario where sample size is fixed per task, and therefore proportional to the number of tasks, $n \propto T$. For detailed calculation of time complexity see Appendix A.3.

Parametric lifelong learning methods have a representational capacity which is invariant to sample size and task number. Although the space complexity of some of these algorithms grow (because the number of the constraints stored by the algorithms grows, or they continue to store more data),

Table 1: Capacity, space, and time complexity of the representation learned by various lifelong learning algorithms. We show soft-O notation ($\tilde{O}(\cdot, \cdot)$ defined in main text) as a function of $n = \sum_t^T n_t$ and T , as well as the common setting where n is proportional to T . The bottom three rows show algorithms whose space and time both grow quasilinearly with capacity growing.

Parametric	Capacity	Space		Time		Examples
	(n, T)	(n, T)	$(n \times T)$	(n, T)	$(n \times T)$	
parametric	1	1	1	1	1	SILLY-N-M, SILLY-F-M
parametric	1	1	1	n	n	O-EWC, SI, LwF
parametric	1	T	n	nT	n^2	EWC
parametric	1	n	n	nT	n^2	TOTAL REPLAY
semi-parametric	T	T^2	n^2	nT	n^2	PROGNN
semi-parametric	T	T	n	n	n	DF-CNN
semi-parametric	T	$T + n$	n	n	n	SILLY-N, MODEL ZOO, DER, LMC
non-parametric	n	n	n	n	n	SILLY-F, IBP-WF

their capacity is fixed. Thus, given a sufficiently large number of tasks with increasing complexity, in general, eventually all parametric methods will catastrophically forget. EWC [10], ONLINE EWC [13], SI [11], and LwF [12] are all examples of parametric lifelong learning algorithms. Our fixed resource algorithms are also parametric. For comparison, we implement another baseline algorithm and refer to it as TOTAL REPLAY, which is also parametric. TOTAL REPLAY replays both old and current task data while learning a new task.

Semi-parametric algorithms’ representational capacity grows slower than sample size. For example, if T is increasing slower than n (e.g., $T \propto \log n$), then algorithms whose capacity is proportional to T are semi-parametric. PROGNN [16] is semi-parametric, nonetheless, its space complexity is $\tilde{O}(T^2)$ due to the lateral connections. Moreover, the time complexity for PROGNN also scales quadratically with n when $n \propto T$. Thus, an algorithm that literally stores all the data it has ever seen, and retrains a fixed size network on all those data with the arrival of each new task, would have smaller space complexity and the same time complexity as PROGNN. DF-CNN [17] improves upon PROGNN by introducing a “knowledge base” with lateral connections to each new column, thereby avoiding all pairwise connections. Because these semi-parametric methods have a fixed representational capacity per task, they will either lack the representation capacity to perform well given sufficiently complex tasks, and/or will waste resources for very simple tasks.

SILLY-N and SILLY-F eliminate the lateral connections between columns of the network, thereby reducing space complexity down to $\tilde{O}(T)$. Moreover, as shown in Figure 3, memory consumed by new channels is negligible compared to that of memory required for storing the encoders. Note that the time required for updating channels is negligible in comparison with the time required for training a new encoder.

Indian Buffet Process for Weight Factors (IBP-WF) is another non-parametric lifelong learning algorithm.

5 Providing intuition of simple lifelong learning through simulations

5.1 Forward and backward transfer in a simple environment

Consider a very simple two-task environment: Gaussian XOR and Gaussian Exclusive NOR (XNOR) (Figure 4A, see Appendix A.4 for details). The two tasks share the exact same discriminant boundaries: the coordinate axes. Thus, transferring from one task to the other merely requires learning a bit flip of the class labels. We sample a total 750 samples from XOR, followed by another 750 samples from XNOR.

SILLY-N and deep network (DN) achieve the same generalization error on XOR when training with XOR data (Figure 4Bi). But because DN does not account for a change in task, when XNOR data appear, DN performance on XOR deteriorates (it catastrophically forgets). In contrast, SILLY-N continues to improve on XOR given XNOR data, demonstrating backward transfer. Now consider the generalization error on XNOR (Figure 4Bii). Both SILLY-N and DN are at chance levels for XNOR when only XOR data are available. When XNOR data are available, DN must unlearn everything it

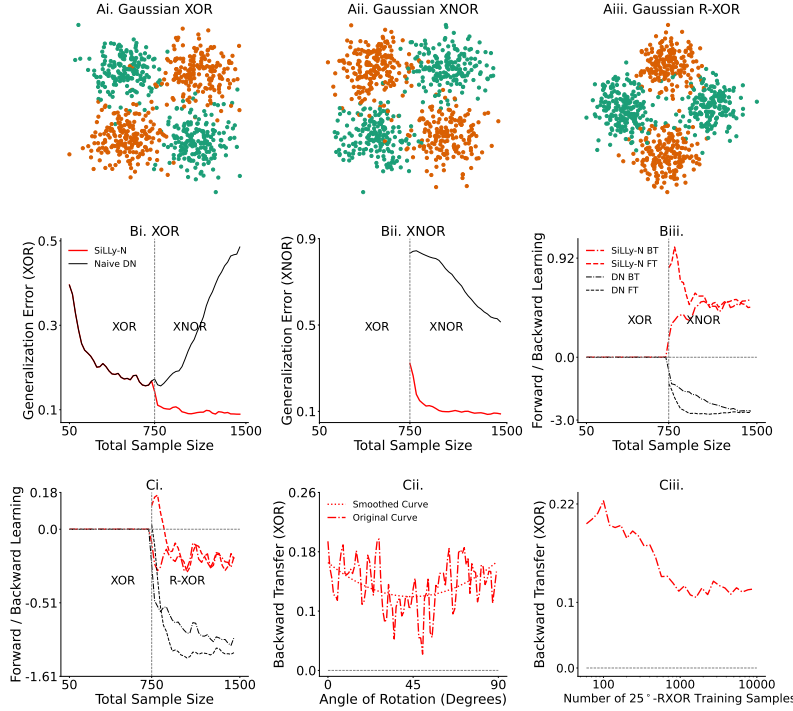


Figure 4: **SILLY-N demonstrates forward and backward transfer.** (A) 750 samples from: (Ai) Gaussian XOR, (Aii) XNOR, which has the same optimal discriminant boundary as XOR, and (Aiii) R-XOR, which has a discriminant boundary that is uninformative, and therefore adversarial, to XOR. (Bi) Generalization error for XOR, and (Bii) XNOR. SILLY-N outperforms DN on XOR when XNOR data is available, and on XNOR when XOR data are available. (Biii) Forward and backward transfer of SILLY-N are positive for all sample sizes. (Ci) In an adversarial task setting, SILLY-N gracefully forgets XOR, whereas DN catastrophically forget and interfere. (Cii) Backward Transfer is maximum positive with respect to XOR when the optimal decision boundary of θ -XOR is similar to that of XOR (e.g. angles far from 45°), and negative otherwise. The dashed line shows the regression line fitted through the original points. (Ciii) Backward Transfer is a nonlinear function of the source training sample size (XOR sample size is fixed at 500).

learned from the XOR data, and thus its performance on XNOR starts out nearly maximally inaccurate, and quickly improves. On the other hand, because SILLY-N can leverage the encoder learned using the XOR data, upon getting *any* XNOR data, it immediately performs quite well, and then continues to improve with further XNOR data, demonstrating forward transfer (Figure 4Biii). SILLY-N demonstrates positive forward and backward transfer for all sample sizes, whereas DN fails to demonstrate neither forward nor backward transfer, and eventually catastrophically forgets the previous tasks.

5.2 Forward and backward transfer for adversarial tasks In the context of lifelong learning, we informally define a task t to be adversarial with respect to task t' if the true joint distribution of task t , without any domain adaptation, impedes performance on task t' . In other words, training data from task t can only add noise, rather than signal, for task t' . An adversarial task for Gaussian XOR is Gaussian XOR rotated by 45° (R-XOR) (Figure 4Aiii). Training on R-XOR therefore impedes the performance of SILLY-N on XOR, and thus backward transfer becomes negative, demonstrating graceful forgetting [44] (Figure 4Ci).

To further investigate this relationship, we design a suite of R-XOR examples, generalizing R-XOR from only 45° to any rotation angle between 0° and 90° , sampling 100 points from XOR, and another 100 from each R-XOR (Figure 4Cii). Note that we could not run the experiment for a lot of Monte Carlo repetition to have a smooth curve and hence we have shown a regressed curve fitted to the low repetition noisy curve. As the angle increases from 0° to 45° , Backward Transfer gradually decreases

for `SILLY-N`. The 45° -XOR is the maximally adversarial R-XOR. Thus, as the angle further increases, Backward Transfer increases back up to ≈ 0.18 at 90° , which has an identical discriminant boundary to XOR. Moreover, when θ is fixed at 25° , Backward Transfer increases at different rates for different sample sizes of the source task (Figure 4Ciii).

Together, these experiments indicate that the amount of transfer can be a complicated function of (i) the difficulty of learning good representations for each task, (ii) the relationship between the two tasks, and (iii) the sample size of each.

6 Benchmark data experiments For benchmark data, we build `SILLY-N` encoders using the network architecture described in [45]. We use the same network architecture for all the benchmarking models. For the following experiments, we consider two modalities of real data: vision and language.

6.1 Reference algorithms We compared our approaches to 15 reference lifelong learning methods. Among them five are resource growing as well as modular approach: `PROGNN` [16], `DF-CNN` [17], `LMC` [46], `MODEL ZOO` [47], `CoSCL` [48]. Note that "MODEL ZOO" was published after our work was archived on arXiv, and the authors have built on our work (personal communications). Other reference algorithms are resource constrained: Elastic Weight Consolidation (EWC) [10], Online-EWC (O-EWC) [13], Synaptic Intelligence (SI) [11], Learning without Forgetting (LwF) [12], and "None".

We also compare two variants of exact replay (Total Replay and Partial Replay) using the code provided in [45]. Both Total and Partial Replay store all the data they have ever seen, but Total Replay replays all of it upon acquiring a new task, whereas Partial Replay replays N samples, randomly sampled from the entire corpus, whenever we acquire a new task with N samples. Additionally, we have compared our approach with more constrained ways of replaying old task data, including Averaged Gradient Episodic Memory (A-GEM) [49], Experience Replay (ER) [50] and Task-based Accumulated Gradients (TAG) [51].

For the baseline "None", the network was incrementally trained on all tasks in the standard way while always only using the data from the current task. The implementations for all of the algorithms are adapted from open source codes [17, 52]; for implementation details, see Appendix A.2.

6.2 Exploring and explaining transfer capabilities via CIFAR 10x10 dataset The CIFAR 100 challenge [53], consists of 50,000 training and 10,000 test samples, each a 32×32 RGB image of a common object, from one of 100 possible classes, such as apples and bicycles. CIFAR 10x10 divides these data into 10 tasks, each with 10 classes [17] (see Appendix A.5 for details).

Resource growing experiments `SILLY-N` and `MODEL ZOO` demonstrate positive forward and backward transfer for every task in CIFAR 10x10, in contrast, other algorithms do not exhibit any positive backward transfer (Figure 1 first column). Moreover, they retained their accuracy while improving transfer (Figure 1, bottom row). `PROGNN` had a similar degree of forward transfer, but zero backward transfer, and requires quadratic space and time in sample size, unlike `SILLY-N` which requires quasilinear space and time.

Ablation experiments Our proposed algorithms can improve performance on all the tasks (past and future) by both growing additional resources and replaying data from the past tasks. Below we do two ablation experiments using CIFAR 10X10 to measure the relative contribution of resource growth and replay on the performance of our proposed algorithms.

Constrained resource experiment In this experiment, we ablate the capability of `SILLY-N` to grow additional resources after learning 4 encoders. We also reduce the number of channels and nodes at each encoder layer by four times to keep the total number of parameters similar to the other constant-resource-algorithms. As shown in the top row of Figure 5, `SILLY-N-4` still shows positive forward and backward transfer with constant resources. However, the accuracy for `SILLY-N-4` gets reduced compared to that of resource growing `SILLY-N` in Figure 1. Note that all the baseline algorithms

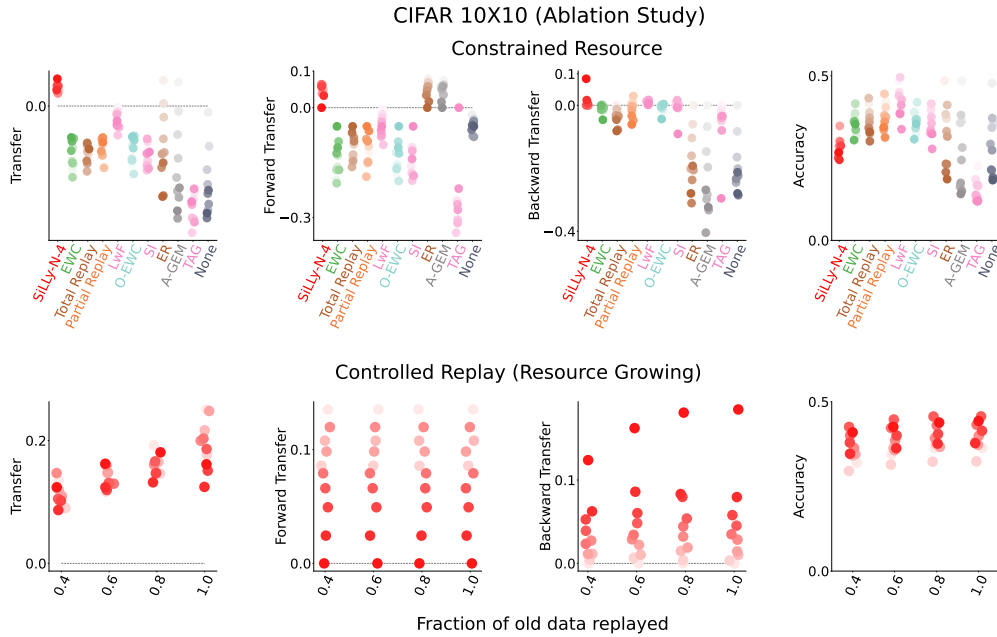


Figure 5: **Ablation experiments on SiLLY-N using CIFAR 10X10.** *Top row:* SiLLY-N uniquely shows both positive forward and backward transfer while operating with the same number of parameters as other baseline constant parameter approaches. *Bottom row:* Replaying old task data impacts backward transfer while keeping forward transfer unchanged for SiLLY-N.

have negative backward transfer. This experiment indicates that constant resource mode operation for SiLLY-N may be advantageous when we have a lot of tasks to learn and have a decent amount of storage budget available. We will elaborate the above point later with a large scale dataset (food1k).

Controlled replay experiment In this experiment, we train four different versions of SiLLY-N sequentially on the 10 tasks from CIFAR 10X10. The only difference between different versions of the algorithms is the amount of old task data replayed. In four different versions of each algorithm, we replay 40%, 60%, 80% and 100% of the old task data respectively. As apparent from Figure 5 bottom, replaying old task data has no effect on forward transfer, but replaying more data improves backward transfer as the number of tasks increases.

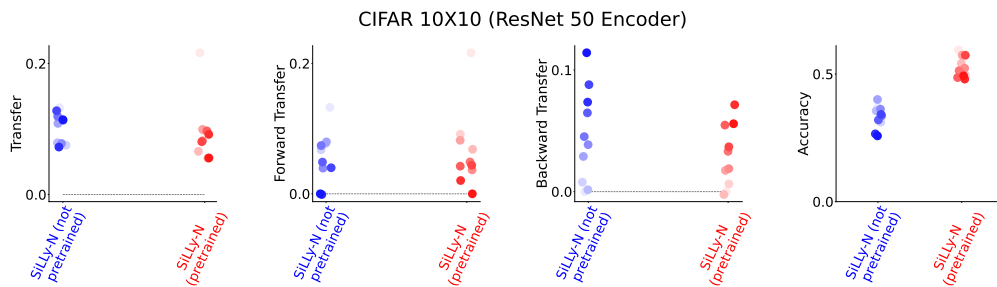


Figure 6: **Pretrained encoder on CIFAR 10X10.** Using pretrained encoders results in better transfer and accuracy for SiLLY-N.

Experiment using pretrained encoders In this experiment, we explore the effect of using pretrained encoders on the performance of SiLLY-N. For this experiment only, we use RESNET 50, as weights for the model pretrained on imagenet dataset is publicly available with the python package: Keras [54]. We initialize the weights of the encoders with the pretrained weights and do not freeze any layer during training. As shown in Figure 6, pretraining the encoders results in better accuracy and forward transfer, but less backward transfer for SiLLY-N. However, as it is unclear how to use pretrained encoders for

other baseline approaches, we do not use pretrained encoders for SiLLy-N in other experiments for fair comparison.

Adversarial experiments Consider the same CIFAR 10x10 experiments above, but, for Task 2 through 9, randomly permute the class labels within each task, rendering each of those tasks adversarial with regard to the first task (because the labels are uninformative). Figure 7A indicates that backward transfer for SiLLy-N show positive backward transfer even with such label shuffling (the other algorithms did not demonstrate positive backward transfer). Now, consider a Rotated CIFAR experiment, which uses only data from the first task, divided into two equally sized subsets (making two tasks), where the second subset is rotated by different amounts (Figure 7, right). Backward transfer of SiLLy-N is nearly invariant to rotation angle, whereas the other approaches are far more sensitive to rotation angle. Note that zero rotation angle corresponds to the two tasks *having identical distributions*. The fact that other algorithms fail to transfer even in this setting suggests that they may not ever be able to positively backwards transfer. See Appendix A.5 for additional experiment using CIFAR 10X10.

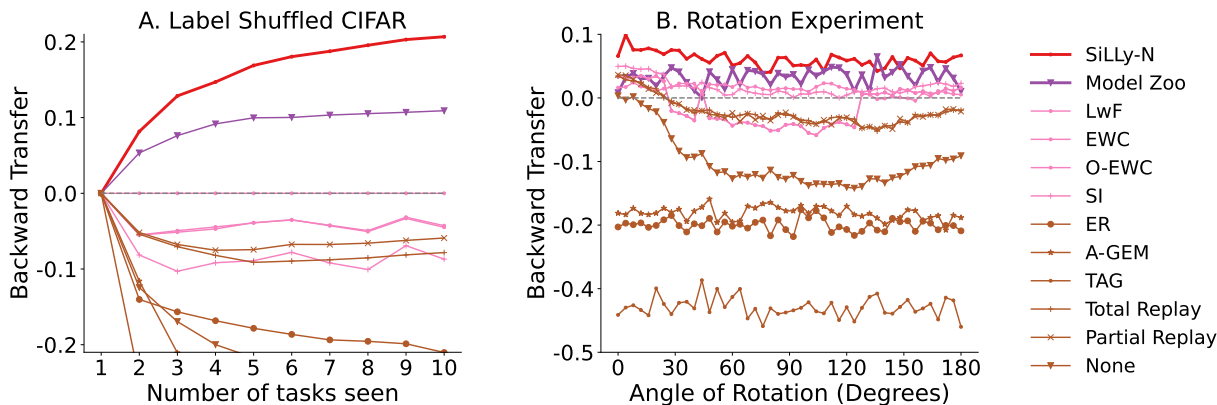


Figure 7: **Extended CIFAR 10x10 experiments.** A. Shuffling class labels within tasks two through nine with 500 samples each demonstrates SiLLy-N can still achieve positive backward transfer, and that the other algorithms still fail to transfer. B. SiLLy-N is nearly invariant to rotations, whereas other approaches are more sensitive to rotation.

6.3 Further investigating transfer in additional datasets with more classes, tasks, and/or samples

Spoken Digit In this experiment, we used the **Spoken Digit** dataset [55]. As shown in Figure 8 first column, SiLLy-N shows positive backward and forward transfer between the spoken digit tasks, in contrast to other methods, some of which show only forward transfer, others show only backward transfer, with none showing both, and some showing neither. See Appendix A.5 for details of the experiment.

FOOD1k 50X20 Dataset In this experiment, we use **Food1k** which is a large scale vision dataset consisting of 1000 food categories from Food2k [56]. FOOD1k 50X20 splits these data into 50 tasks with 20 classes each. For each class, we randomly sampled 60 samples per class for training the models and used rest of the data for testing purpose. Because on the CIFAR experiments MODEL ZOO performs the best among the reference resource growing models, and LwF is the best performing resource constrained algorithm, we only use them as the reference models for the large scale experiment to avoid heavy computational cost. As shown in Figure 8 second column, SiLLy-N performs the best among all the algorithms on this large dataset.

In lifelong learning, we are often primarily concerned with situations in which we have a small number of samples per task. If we have enough samples per tasks, the learning agent need not transfer knowledge from other tasks. However, below we also experiment with non-trivial lifelong learning setting

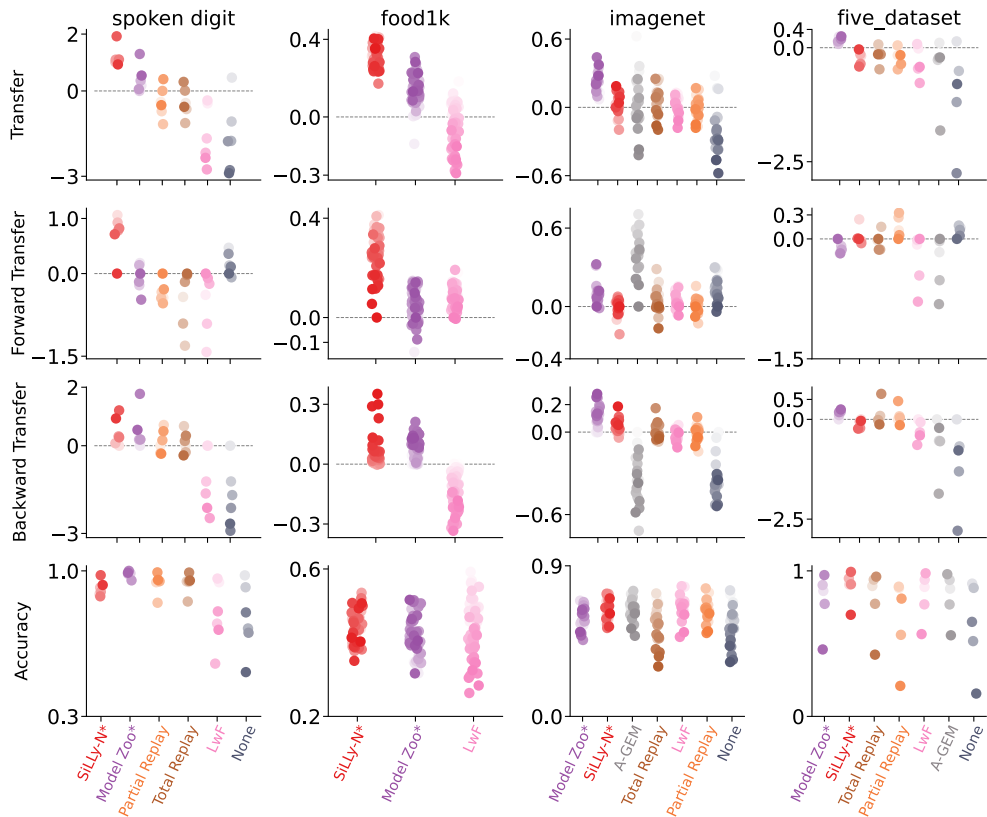


Figure 8: **Performance summary on vision and speech benchmark datasets with varying sample sizes per task.** Dataset on the right has more samples per task. Imagenet and five dataset have really high sample size per task which is a non-trivial lifelong learning setting. SiLLy-N performs the best in the low sample size regime on the left two columns which is desirable in lifelong learning. See appendix Figure 3 and 5 for the extended results.

where sample per task is high.

Split Mini-Imagenet In this experiment, we have used the **Mini-Imagenet** dataset [51]. The dataset was split into 20 tasks with 5 classes each. Each task has 2400 training samples and 600 testing samples. As shown in Figure 1 fourth column, we get positive forward and backward transfer for SiLLy-N. However, although samples per task is lower compared to that of 5-dataset, it is still quite high. Hence, Model Zoo outperforms all the algorithms in this experiment.

5-dataset In this experiment, we have used **5-dataset** [51]. It consists of 5 tasks from five different datasets: CIFAR-10 [53], MNIST, SVHN [57], notMNIST [58], Fashion-MNIST [59]. All the monochromatic images were converted to RGB format, and then resized to $3 \times 32 \times 32$. As shown in Appendix Table 3, training samples per task in 5-dataset is relatively higher than that of low data regime typically considered in lifelong learning setting. However, as shown in Figure 8 fourth column, SiLLy-N show less forgetting than most of the reference algorithms. On the other hand, Model Zoo shows comparatively better performance in relatively high task data size setup. Recall that SiLLy-N is based on bagging, and Model Zoo is based on boosting. It is well known that boosting often outperforms bagging when sample sizes are large ².

²Authors in [60] shows that both bagging and boosting asymptotically converge to the Bayes optimal solution. However, for finite sample size and similar model complexity, we empirically find bagging approach to lifelong learning performs better than that of boosting when the training sample size is low whereas boosting performs better on large training sample size (See Figure 1 and 8). This is consistent with similar results in single task learning [25, 61, 62]

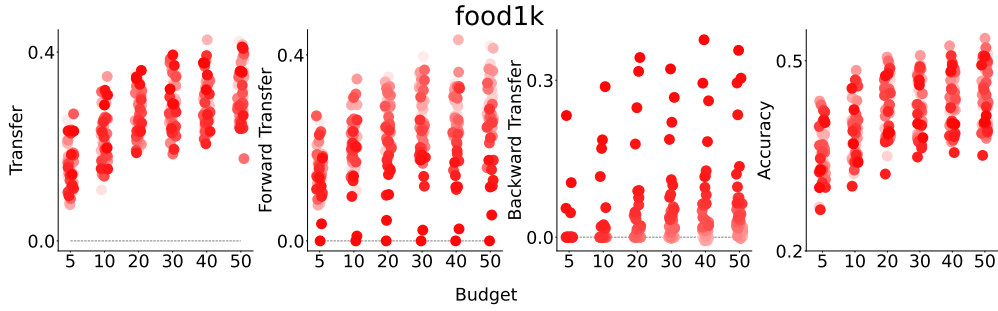


Figure 9: SiLLY-N in constant resource mode operation. Improvement in Transfer between tasks becomes negligible at nearly 30 encoders. The user can choose to operate in lower budget with less transfer.

6.4 Constant Resource Mode Operation The binary distinction we made above, algorithms either build resources or reallocate them, is a false dichotomy, and biologically unnatural. In biological learning, systems develop from building to fixed resources, as they grow from juveniles to adults. To explore this continuum of amount of resources to grow, we experiment on FOOD1k 50X20 dataset using the constant resource mode operation of SiLLY-N as described in Section 3. We evaluate the performance of SiLLY-N for different number of encoder budget. As shown in Figure 9, performance of SiLLY-N saturates after 30 encoders, though with only 5 encoders, still demonstrates forward and backward transfer.

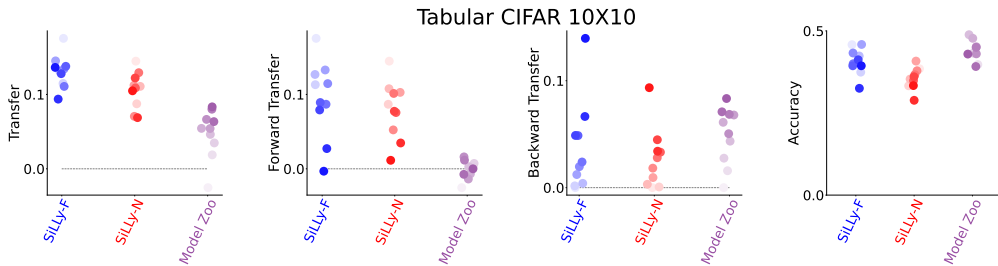


Figure 10: Our proposed approach can be used with random forest as encoders on tabular data (SiLLY-F). SiLLY-F shows more positive forward and backward transfer while operating with less parameters compared to other baseline approaches on tabular data.

7 SiLLY-F on tabular data In this experiment, we experiment with SiLLY-F, an additional realization of our approach using random forests as encoders (described in Section 3). We flatten the CIFAR 10X10 data and use them as tabular data. We train two other best performing baseline algorithms, SiLLY-N and Model Zoo and use three fully connected hidden layers, each having 2000 nodes, as encoders. As shown in Figure 10, SiLLY-F performs the best among all the approaches. This experiment shows our approach can be used as a general structure to do lifelong learning using other machine learning models as encoder.

8 Discussion We introduced representation ensembling as a simple approach for lifelong learning. Two specific algorithms, SiLLY-N and SiLLY-F, achieve both forward and backward transfer, by leveraging resources learned for other tasks without undue computational burdens. In this paper, we have mainly focused on task-aware setting, because it is simpler. Future work will extend our approach to more challenging task-unaware settings. Our code, including code to reproduce the experiments in this manuscript, is available from <http://proglearn.neurodata.io/>.

Acknowledgements The authors thank the support of the NSF-Simons Research Collaborations on the Mathematical and Scientific Foundations of Deep Learning (NSF grant 2031985). We also thank Raman Arora, Dinesh Jayaraman, Rene Vidal, Jeremias Sulam, Guillermo Sapiro, and Michael Pow-

ell for helpful discussions. This work is graciously supported by the Defense Advanced Research Projects Agency (DARPA) Lifelong Learning Machines program through contracts FA8650-18-2-7834 and HR0011-18-2-0025. Research was partially supported by funding from Microsoft Research and the Kavli Neuroscience Discovery Institute.

References

- [1] Tom M Mitchell. Machine learning and data mining. *Communications of the ACM*, 42(11):30–36, 1999.
- [2] V Vapnik and A Chervonenkis. On the Uniform Convergence of Relative Frequencies of Events to Their Probabilities. *Theory Probab. Appl.*, 16(2):264–280, January 1971.
- [3] L G Valiant. A Theory of the Learnable. *Commun. ACM*, 27(11):1134–1142, November 1984. URL <http://doi.acm.org/10.1145/1968.1972>.
- [4] Rich Caruana. Multitask learning. *Machine learning*, 28(1):41–75, 1997.
- [5] Sebastian Thrun. Is learning the n-th thing any easier than learning the first? In *Advances in neural information processing systems*, pages 640–646, 1996.
- [6] Sebastian Thrun and Lorien Pratt. *Learning to Learn*. Springer Science & Business Media, December 2012. URL https://market.android.com/details?id=book-X_jpBwAAQBAJ.
- [7] Michael McCloskey and Neal J Cohen. Catastrophic interference in connectionist networks: The sequential learning problem. In *Psychology of learning and motivation*, volume 24, pages 109–165. Elsevier, 1989.
- [8] James L McClelland, Bruce L McNaughton, and Randall C O’Reilly. Why there are complementary learning systems in the hippocampus and neocortex: insights from the successes and failures of connectionist models of learning and memory. *Psychological review*, 102(3):419, 1995.
- [9] Jing Zhao, Blanca Quiroz, L Quentin Dixon, and R Malatesha Joshi. Comparing Bilingual to Monolingual Learners on English Spelling: A Meta-analytic Review. *Dyslexia*, 22(3):193–213, August 2016.
- [10] James Kirkpatrick, Razvan Pascanu, Neil Rabinowitz, Joel Veness, Guillaume Desjardins, Andrei A Rusu, Kieran Milan, John Quan, Tiago Ramalho, Agnieszka Grabska-Barwinska, Demis Hassabis, Claudia Clopath, Dharshan Kumaran, and Raia Hadsell. Overcoming catastrophic forgetting in neural networks. *Proceedings of the national academy of sciences*, 114(13):3521–3526, 2017.
- [11] Friedemann Zenke, Ben Poole, and Surya Ganguli. Continual learning through synaptic intelligence. In *Proceedings of the 34th International Conference on Machine Learning-Volume 70*, pages 3987–3995. JMLR. org, 2017.
- [12] Zhizhong Li and Derek Hoiem. Learning without forgetting. *IEEE transactions on pattern analysis and machine intelligence*, 40(12):2935–2947, 2017.
- [13] Jonathan Schwarz, Jelena Luketina, Wojciech M Czarnecki, Agnieszka Grabska-Barwinska, Yee Whye Teh, Razvan Pascanu, and Raia Hadsell. Progress & compress: A scalable framework for continual learning. *arXiv preprint arXiv:1805.06370*, 2018.
- [14] Chelsea Finn, Aravind Rajeswaran, Sham Kakade, and Sergey Levine. Online meta-learning. In Kamalika Chaudhuri and Ruslan Salakhutdinov, editors, *International Conference on Machine Learning*, volume 97 of *Proceedings of Machine Learning Research*, pages 1920–1930, Long Beach, California, USA, 06 2019. PMLR. URL <http://proceedings.mlr.press/v97/finn19a.html>.
- [15] Paul Ruvolo and Eric Eaton. ELLA: An Efficient Lifelong Learning Algorithm. In *International Conference on Machine Learning*, volume 28, pages 507–515, February 2013. URL <http://proceedings.mlr.press/v28/ruvolo13.html>.
- [16] Andrei A Rusu, Neil C Rabinowitz, Guillaume Desjardins, Hubert Soyer, James Kirkpatrick, Koray Kavukcuoglu, Razvan Pascanu, and Raia Hadsell. Progressive neural networks. *arXiv preprint arXiv:1606.04671*, 2016.

- [17] Seungwon Lee, James Stokes, and Eric Eaton. Learning shared knowledge for deep lifelong learning using deconvolutional networks. In Proceedings of the 28th International Joint Conference on Artificial Intelligence, pages 2837–2844, 2019.
- [18] Shagun Sodhani, Sarath Chandar, and Yoshua Bengio. Toward training recurrent neural networks for lifelong learning. Neural computation, 32(1):1–35, 2020.
- [19] German I Parisi, Ronald Kemker, Jose L Part, Christopher Kanan, and Stefan Wermter. Continual lifelong learning with neural networks: A review. Neural Networks, 2019.
- [20] Zhiyuan Chen and Bing Liu. Lifelong Machine Learning. Synthesis Lectures on Artificial Intelligence and Machine Learning, 10(3):1–145, November 2016. URL <https://doi.org/10.2200/S00737ED1V01Y201610AIM033>.
- [21] Judea Pearl. The seven tools of causal inference, with reflections on machine learning. Commun. ACM, February 2019.
- [22] Gary Marcus and Ernest Davis. Rebooting AI: Building Artificial Intelligence We Can Trust. Pantheon, September 2019.
- [23] David Lopez-Paz and Marc’Aurelio Ranzato. Gradient episodic memory for continual learning. In NIPS, 2017.
- [24] Diana Benavides-Prado, Yun Sing Koh, and Patricia Riddle. Measuring Cumulative Gain of Knowledgeable Lifelong Learners. In NeurIPS Continual Learning Workshop, pages 1–8, 2018.
- [25] Natalia Díaz-Rodríguez, Vincenzo Lomonaco, David Filliat, and Davide Maltoni. Don’t forget, there is more than forgetting: new metrics for continual learning. arXiv preprint arXiv:1810.13166, 2018.
- [26] Tom Veniat, Ludovic Denoyer, and Marc’Aurelio Ranzato. Efficient continual learning with modular networks and task-driven priors. arXiv preprint arXiv:2012.12631, 2020.
- [27] Pearl Judea. What is gained from past learning. Journal of Causal Inference, 6(1), 2018.
- [28] Peter J Bickel and Kjell A Doksum. Mathematical statistics: basic ideas and selected topics, volumes I-II package. Chapman and Hall/CRC, 2015.
- [29] Thomas M Cover and Joy A Thomas. Elements of Information Theory. John Wiley & Sons, New York, November 2012.
- [30] Kyunghyun Cho, B van Merriënboer, Caglar Gulcehre, F Bougares, H Schwenk, and Yoshua Bengio. Learning phrase representations using rnn encoder-decoder for statistical machine translation. In Conference on Empirical Methods in Natural Language Processing (EMNLP 2014), 2014.
- [31] Ashish Vaswani, Noam Shazeer, Niki Parmar, Jakob Uszkoreit, Llion Jones, Aidan N Gomez, Łukasz Kaiser, and Illia Polosukhin. Attention is All you Need. In I Guyon, U V Luxburg, S Bengio, H Wallach, R Fergus, S Vishwanathan, and R Garnett, editors, Advances in Neural Information Processing Systems 30, pages 5998–6008. Curran Associates, Inc., 2017.
- [32] Jacob Devlin, Ming-Wei Chang, Kenton Lee, and Kristina Toutanova. BERT: pre-training of deep bidirectional transformers for language understanding. CoRR, abs/1810.04805, 2018. URL <http://arxiv.org/abs/1810.04805>.
- [33] Leo Breiman, Jerome Friedman, Charles J Stone, and Richard A Olshen. Classification and regression trees. CRC press, 1984.
- [34] M. Denil, D. Matheson, and N. De Freitas. Narrowing the gap: Random forests in theory and in practice. In Eric P. Xing and Tony Jebara, editors, Proceedings of the 31st International Conference on Machine Learning, volume 32 of Proceedings of Machine Learning Research, pages 665–673, 6 2014.
- [35] S. Athey, J. Tibshirani, and S. Wager. Generalized random forests. Annals of Statistics, 47(2): 1148–1178, 2019.
- [36] Leo Breiman. Bagging predictors. Mach. Learn., 24(2):123–140, August 1996.
- [37] Y Freund. Boosting a Weak Learning Algorithm by Majority. Inform. and Comput., 121(2):256–285, September 1995.

- [38] Leo Breiman. Random forests. *Machine learning*, 45(1):5–32, 2001.
- [39] Charles J Stone. Consistent Nonparametric Regression. *Ann. Stat.*, 5(4):595–620, July 1977.
- [40] Yali Amit and Donald Geman. Shape Quantization and Recognition with Randomized Trees. *Neural Comput.*, 9(7):1545–1588, October 1997.
- [41] Way Kuo and Ming J Zuo. *Optimal reliability modeling: principles and applications*. John Wiley & Sons, 2003.
- [42] Chiyuan Zhang, Samy Bengio, Moritz Hardt, Benjamin Recht, and Oriol Vinyals. Understanding deep learning (still) requires rethinking generalization. *Communications of the ACM*, 64(3):107–115, 2021.
- [43] Iris van Rooij, Mark Blokpoel, Johan Kwisthout, and Todd Wareham. *Cognition and Intractability: A Guide to Classical and Parameterized Complexity Analysis*. Cambridge University Press, April 2019.
- [44] Rahaf Aljundi, Francesca Babiloni, Mohamed Elhoseiny, Marcus Rohrbach, and Tinne Tuytelaars. Memory aware synapses: Learning what (not) to forget. In Vittorio Ferrari, Martial Hebert, Cristian Sminchisescu, and Yair Weiss, editors, *Computer Vision – ECCV 2018*, pages 144–161, Cham, 2018. Springer International Publishing.
- [45] Gido M van de Ven, Hava T Siegelmann, and Andreas S Tolias. Brain-inspired replay for continual learning with artificial neural networks. *Nature communications*, 11:4069, 2020.
- [46] Oleksiy Ostapenko, Pau Rodriguez, Massimo Caccia, and Laurent Charlin. Continual learning via local module composition. *Advances in Neural Information Processing Systems*, 34:30298–30312, 2021.
- [47] Rahul Ramesh and Pratik Chaudhari. Model zoo: A growing brain that learns continually. In *International Conference on Learning Representations*, 2021.
- [48] Liyuan Wang, Xingxing Zhang, Qian Li, Jun Zhu, and Yi Zhong. Coscl: Cooperation of small continual learners is stronger than a big one. In *European Conference on Computer Vision*, pages 254–271. Springer, 2022.
- [49] Arslan Chaudhry, Marc’Aurelio Ranzato, Marcus Rohrbach, and Mohamed Elhoseiny. Efficient lifelong learning with a-gem. *arXiv preprint arXiv:1812.00420*, 2018.
- [50] Arslan Chaudhry, Marcus Rohrbach, Mohamed Elhoseiny, Thalaiyasingam Ajanthan, Puneet K Dokania, Philip HS Torr, and Marc’Aurelio Ranzato. On tiny episodic memories in continual learning. *arXiv preprint arXiv:1902.10486*, 2019.
- [51] Pranshu Malviya, Sarath Chandar, and Balaraman Ravindran. Tag: Task-based accumulated gradients for lifelong learning. *arXiv preprint arXiv:2105.05155*, 2021.
- [52] Gido M. van de Ven and Andreas S. Tolias. Three scenarios for continual learning. *CoRR*, abs/1904.07734, 2019. URL <http://arxiv.org/abs/1904.07734>.
- [53] Alex Krizhevsky. Learning multiple layers of features from tiny images. *University of Toronto*, 05 2012.
- [54] François Chollet et al. Keras. <https://github.com/fchollet/keras>, 2015.
- [55] Zohar Jackson, César Souza, Jason Flaks, Yuxin Pan, Hereman Nicolas, and Adhish Thite. Jakobovski/free-spoken-digit-dataset: v1. 0.8. *Zenodo*, August, 2018.
- [56] Weiqing Min, Zhiling Wang, Yuxin Liu, Mengjiang Luo, Liping Kang, Xiaoming Wei, Xiaolin Wei, and Shuqiang Jiang. Large scale visual food recognition. *CoRR*, abs/2103.16107, 2021.
- [57] Yuval Netzer, Tao Wang, Adam Coates, Alessandro Bissacco, Bo Wu, and Andrew Y Ng. Reading digits in natural images with unsupervised feature learning. 2011.
- [58] Yaroslav Bulatov. <http://yaroslavvb.blogspot.com/2011/09/notmnist-dataset.html>. 2011.
- [59] Han Xiao, Kashif Rasul, and Roland Vollgraf. Fashion-mnist: a novel image dataset for benchmarking machine learning algorithms. *arXiv preprint arXiv:1708.07747*, 2017.
- [60] Abraham J Wyner, Matthew Olson, Justin Bleich, and David Mease. Explaining the success of adaboost and random forests as interpolating classifiers. *The Journal of Machine Learning Research*,

- 18(1):1558–1590, 2017.
- [61] Rich Caruana and Alexandru Niculescu-Mizil. An Empirical Comparison of Supervised Learning Algorithms. In Proceedings of the 23rd International Conference on Machine Learning, ICML '06, pages 161–168, New York, NY, USA, 2006. ACM.
- [62] Rich Caruana, Alexandru Niculescu-Mizil, Geoff Crew, and Alex Ksikes. Ensemble selection from libraries of models. In Proceedings of the twenty-first international conference on Machine learning, page 18, 2004.
- [63] Tianqi Chen and Carlos Guestrin. XGBoost: A Scalable Tree Boosting System. In Proceedings of the 22nd ACM SIGKDD International Conference on Knowledge Discovery and Data Mining, KDD '16, pages 785–794, New York, NY, USA, August 2016. Association for Computing Machinery.
- [64] Xueheng Qiu, Le Zhang, Ye Ren, Ponnuthurai N Suganthan, and Gehan Amaratunga. Ensemble deep learning for regression and time series forecasting. In 2014 IEEE symposium on computational intelligence in ensemble learning (CIEL), pages 1–6. IEEE, 2014.
- [65] Cristhian Potes, Saman Parvaneh, Asif Rahman, and Bryan Conroy. Ensemble of feature-based and deep learning-based classifiers for detection of abnormal heart sounds. In 2016 computing in cardiology conference (CinC), pages 621–624. IEEE, 2016.
- [66] Haixun Wang, Wei Fan, Philip S Yu, and Jiawei Han. Mining concept-drifting data streams using ensemble classifiers. In Proceedings of the ninth ACM SIGKDD international conference on Knowledge discovery and data mining, pages 226–235, 2003.
- [67] Wenyuan Dai, Qiang Yang, Gui-Rong Xue, and Yong Yu. Boosting for transfer learning.(2007), 193–200. In Proceedings of the 24th international conference on Machine learning, 2007.
- [68] Robi Polikar, Lalita Upda, Satish S Upda, and Vasant Honavar. Learn++: An incremental learning algorithm for supervised neural networks. IEEE transactions on systems, man, and cybernetics, part C (applications and reviews), 31(4):497–508, 2001.
- [69] Gido M van de Ven, Tinne Tuytelaars, and Andreas S Tolias. Three types of incremental learning. Nature Machine Intelligence, pages 1–13, 2022.
- [70] Arun Mallya and Svetlana Lazebnik. Packnet: Adding multiple tasks to a single network by iterative pruning. In Proceedings of the IEEE conference on Computer Vision and Pattern Recognition, pages 7765–7773, 2018.
- [71] Nikhil Mehta, Kevin Liang, Vinay Kumar Verma, and Lawrence Carin. Continual learning using a bayesian nonparametric dictionary of weight factors. In International Conference on Artificial Intelligence and Statistics, pages 100–108. PMLR, 2021.
- [72] Shipeng Yan, Jiangwei Xie, and Xuming He. Der: Dynamically expandable representation for class incremental learning. In Proceedings of the IEEE/CVF Conference on Computer Vision and Pattern Recognition, pages 3014–3023, 2021.
- [73] Anthony Robins. Catastrophic forgetting, rehearsal and pseudorehearsal. Connection Science, 7(2):123–146, 1995.
- [74] Hanul Shin, Jung Kwon Lee, Jaehong Kim, and Jiwon Kim. Continual learning with deep generative replay. In Advances in Neural Information Processing Systems, pages 2990–2999, 2017.
- [75] Rich Caruana, Nikos Karampatziakis, and Ainur Yessenalina. An empirical evaluation of supervised learning in high dimensions. In Proceedings of the 25th international conference on Machine learning, pages 96–103, New York, New York, USA, July 2008. ACM.
- [76] Manuel Fernández-Delgado, Eva Cernadas, Senén Barro, and Dinani Amorim. Do we need hundreds of classifiers to solve real world classification problems. J. Mach. Learn. Res., 15(1):3133–3181, 2014.

.1 Literature review Prior work illustrates that ensembling learners can yield huge advantages in a wide range of applications. For example, in classical machine learning, ensembling trees leads to state-of-the-art random forest [38] and gradient boosting tree algorithms [63]. Similarly, ensembling networks shows promising results in various real-world applications [64, 65]. Authors from [66] used weighted ensemble of learners in a streaming setting with distribution shift. `TRADABOOST` [67] boosts ensemble of learners to enable transfer learning. In continual learning scenarios, many algorithms have been built on these ideas by ensembling dependent representations. For example, `LEARN++` [68] boosts ensembles of weak learners learned over different data sequences in class incremental lifelong learning settings [69]. `MODEL ZOO` [47] uses the same boosting approach in task incremental lifelong learning scenarios.

Another group of algorithms, `PROGNN` [16] and `DF-CNN` [17] learn a new “column” of nodes and edges with each new task, and ensembles the columns for inference (such approaches are commonly called ‘modular’ now). The primary difference between `PROGNN` and `DF-CNN` is that `PROGNN` has forward connections to the current column from all the past columns. This creates the possibility of forward transfer while freezing backward transfer. However, the forward connections in `PROGNN` render it computationally inefficient for a large number of tasks. `DF-CNN` gets around this problem by learning a common knowledge base and thereby, creating the possibility of backward transfer.

Recently, many other modular approaches have been proposed in the literature that improve on `PROGNN`’s capacity growth. These methods consider the capacity for each task being composed of modules that can be shared across tasks and grown as necessary. For example, `PACKNET` [70] starts with a fixed capacity network and trains for additional tasks by freeing up portion of the network capacity using iterative pruning. `Veniat` [26] trains additional modules with each new task, and the old modules are only used selectively. Another paper [46] improved the memory efficiency of the modular methods by adding new modules according to the complexity of the new tasks. Authors in [71] proposed non-parametric factorization of the layer weights that promotes sharing of the weights between tasks. However, all of modular methods described above lack backward transfer because the old modules are not updated with the new tasks. Dynamically Expandable Representation (`DER`) [72] proposed an improvement over the modular approaches where the model capacity is dynamically expanded and the model is fine-tuned by replaying a portion of the old task data along with the new task data. This approach achieves backward transfer between tasks as reported by the authors in the experiments.

Another strategy for building lifelong learning machines is to use total or partial replay [45, 73, 74]. Replay approaches keep the old data and replay them when faced with new tasks to mitigate catastrophic forgetting. However, as we will illustrate, previously proposed replay algorithms do not demonstrate positive backward transfer in our experiments, though they often do not forget as much as other approaches.

Our approach builds directly on previously proposed modular and replay approaches with one key distinction: in our approach, representations are learned independently. Empirically, for low sample sizes random forests (which learn independent trees) typically outperform gradient boosted trees (which learn dependent trees) [62, 75, 76]. Because our approach of representation ensembling is similar to that of random forest, we expect learning independent representations to outperform learning dependent representations in these scenarios as well. This phenomenon is empirically shown in the main text Figure 1 and 8. Independent representations also have computational advantages, as doing so merely requires quasilinear time and space, and can be learned in parallel.

Appendix A. Evaluation Criteria.

A.1 Representation Ensembling Algorithms In this paper, we have proposed two representation ensembling algorithms, Simple Lifelong Learning Networks (`SILLY-N`) and Simple Lifelong Learning Forests (`SILLY-F`). The two algorithms differ in their details of how to update encoders and channels, but abstracting a level up they are both special cases of the same procedure. Let `SILLY-X` refer to any

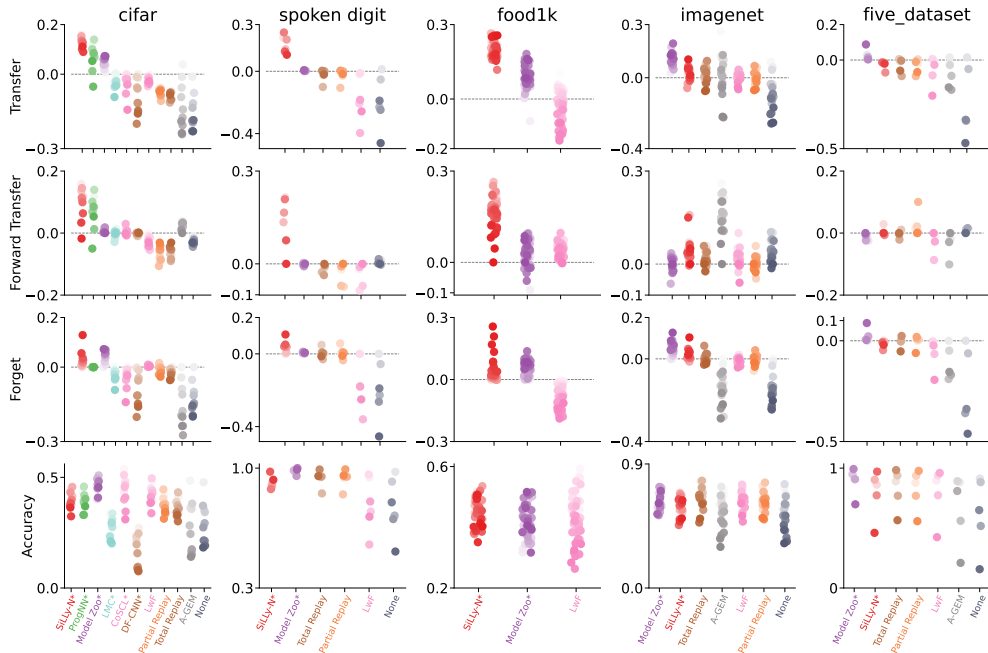


Figure 1: **Performance summary on vision and audition benchmark datasets using Veniat’s [26]’s statistics.** See Figure 1 for caption details. Note that the results here look nearly identical other than the y-axis labels.

possible representation algorithm. Algorithms 1, 2, 3, and 4 provide pseudocode for adding encoders, updating channels, and making predictions for any SiLLy-X algorithm. Whenever the learner gets access to a new task data, we use Algorithm 1 to train a new encoder for the corresponding task. We split the data into two portions — one set is used to learn the encoder and the other portion is called the held out or out-of-bag (OOB) data which is returned by Algorithm 1 to be used by Algorithm 2 to learn the channel for the corresponding task. Note that we push the OOB data through the in-task encoder and the whole dataset through the cross-task encoders to update the channel, i.e, learn the posteriors according to the new encoder. Then we use Algorithm 3 to replay the old task data through the new encoder and update their corresponding channels. Finally, while predicting for a test sample, we use Algorithm 4. Given the task identity, we use the corresponding channel to get the average estimated posterior and predict the class label as the argmax of the estimated posteriors.

Algorithm 1 Add a new SiLLy-X encoder for a task. OOB = out-of-bag.

Input:

- (1) t ▷ current task number
- (2) $\mathcal{D}_n^t = (\mathbf{x}^t, \mathbf{y}^t) \in \mathbb{R}^{n \times p} \times \{1, \dots, K\}^n$ ▷ training data for task t

Output:

- (1) u_t ▷ an encoder trained on task t
 - (2) \mathcal{I}_{OOB}^t ▷ a set of the indices of OOB data
- 1: **function** SiLLy-X.FIT($t, (\mathbf{x}^t, \mathbf{y}^t)$)
 - 2: $u_t, \mathcal{I}_{OOB}^t \leftarrow \text{encoder.fit}(\mathbf{x}^t, \mathbf{y}^t)$ ▷ train an encoder on training data partitioned into in-bag and OOB samples
 - 3: **return** u_t, \mathcal{I}_{OOB}^t
 - 4: **end function**
-

Algorithm 2 Add a new SILLY-X channel for the current task.

Input:

- (1) t ▷ current task number
- (2) $\mathcal{U} = \{u_{t'}\}_{t'=1}^t$ ▷ the set of encoders
- (3) $\mathcal{D}_n^t = (\mathbf{x}^t, \mathbf{y}^t) \in \mathbb{R}^{n \times p} \times \{1, \dots, K\}^n$ ▷ training data for task t
- (4) \mathcal{I}_{OOB}^t ▷ a set of the indices of OOB data for the current task

Output: v_t ▷ channel for task t

- 1: **function** SILLY-X.ADD_CHANNEL($t, u_t, (\mathbf{x}_t, \mathbf{y}_t), \mathcal{I}_{OOB}^t$)
 - 2: $v_t \leftarrow u_t.add_channel((\mathbf{x}_t, \mathbf{y}_t), \mathcal{I}_{OOB}^t)$ ▷ add the new in-task channel using OOB data
 - 3: **for** $t' = 1, \dots, t - 1$ **do**
 - 4: $v_t \leftarrow u_{t'}.update_channel(\mathbf{x}_t, \mathbf{y}_t, v_t)$ ▷ update the channel for task t using the old encoders
 - 5: **end for**
 - 6: **return** v_t
 - 7: **end function**
-

Algorithm 3 Update SILLY-X channel for the previous tasks.

Input:

- (1) t ▷ current task number
- (2) u_t ▷ encoder for the current task
- (3) $\mathcal{D} = \{\mathcal{D}^{t'}\}_{t'=1}^{t-1}$ ▷ training data for old tasks
- (4) $\mathcal{V} = \{v_{t'}\}_{t'=1}^{t-1}$ ▷ set of all previous task voters

Output: $\mathcal{V} = \{v_{t'}\}_{t'=1}^{t-1}$

- 1: **function** SILLY-X.UPDATE_CHANNEL($t, u_t, \mathcal{D}, \mathcal{V}$)
 - 2: **for** $t' = 1, \dots, t - 1$ **do**
 - 3: $v_{t'} \leftarrow u_t.update_channel(\mathbf{x}_{t'}, \mathbf{y}_{t'}, v_{t'})$ ▷ update the old task channels
 - 4: **end for**
 - 5: **return** \mathcal{V}
 - 6: **end function**
-

Algorithm 4 Predicting a class label using SYNX.

Input:

- (1) $\mathbf{x} \in \mathbb{R}^p$ ▷ test datum
- (2) t ▷ task identity associated with \mathbf{x}
- (3) \mathcal{U} ▷ set of all t encoders
- (4) v_t ▷ channel for task t

Output: \hat{y} ▷ a predicted class label

- 1: **function** $\hat{y} =$ SILLY-X.PREDICT(t, \mathbf{x}, v_t)
 - 2: **for** $t' = 1, \dots, t$ **do** ▷ get the output $\tilde{\mathbf{x}} = \{\tilde{\mathbf{x}}_{t'}\}_{t'=1}^t$ from all the encoders
 - 3: $\tilde{\mathbf{x}}_{t'} \leftarrow u_{t'}.encode(\mathbf{x})$
 - 4: **end for**
 - 5: $\hat{\mathbf{p}} \leftarrow v_t.predict_proba(\tilde{\mathbf{x}})$ ▷ $\hat{\mathbf{p}}$ is a K_t -dimensional posterior vector
 - 6: $\hat{y} = \text{argmax}(\hat{\mathbf{p}})$ ▷ find the index of the elements in the vector $\hat{\mathbf{p}}$ with maximum value
 - 7: **return** \hat{y}
 - 8: **end function**
-

Table 1: Hyperparameters for SILLY-N in CIFAR 10X10, Five Datasets, Split Mini-Imagenet, FOOD1k experiments. Note that we use the same hyperparameters for all the experiments.

Hyperparameters	Value
optimizer	Adam
learning rate	3×10^{-4}
max_samples (OOB split)	0.67
K (KNN channel)	$\log_2(\text{number of samples per task})$

Table 2: Hyperparameters for SILLY-F in tabular CIFAR 10X10 experiments.

Hyperparameters	Value
n_estimators	10
max_depth	30
max_samples (OOB split)	0.67
min_samples_leaf	1

A.2 Reference Algorithm Implementation Details The same network architecture was used for all baseline deep learning methods. Following the work in [45], the ‘base network architecture’ consisted of five convolutional layers followed by two-fully connected layers each containing 2000 nodes with ReLU non-linearities and a softmax output layer. The convolutional layers had 16, 32, 64, 128 and 254 channels, they used batch-norm and a ReLU non-linearity, they had a 3x3 kernel, a padding of 1 and a stride of 2 (except the first layer, which had a stride of 1). This architecture was used with a multi-headed output layer (i.e., a different output layer for each task) for all algorithms using a fixed-size network. For ProgNN and DF-CNN the same architecture was used for each column introduced for each new task, and in our SILLY-N this architecture was used for the transformers u_t (see above). In these implementations, ProgNN and DF-CNN have the same architecture for each column introduced for each task. Among the reference algorithms, EWC, O-EWC, LwF, SI, TOTAL REPLAY and PARTIAL REPLAY results were produced using the repository <https://github.com/GMvandeVen/progressive-learning-pytorch>. For ProgNN and DF-CNN we used the code provided in <https://github.com/Lifelong-ML/DF-CNN>. For all other reference algorithms, we modified the code provided by the authors to match the deep net architecture as mentioned above and used the default hyperparameters provided in the code.

A.3 Training Time Complexity Analysis Consider a lifelong learning environment with T tasks each with n' samples, i.e., total training samples, $n = n'T$. For all the algorithm with time complexity $\tilde{O}(n)$, the training time grows linearly with more training samples. We discuss all other algorithms with non-linear time complexity below.

EWC Consider the time required to train the weights for each task in EWC is $k_c n'$ and each task adds additional $k_l n'$ time from the regularization term. Here, k_c and k_l are both constants. Therefore, time required to learn all the T tasks can be written as:

$$\begin{aligned}
& k_c n' + (k_c n' + k_l n') + \dots + (k_c n' + (T-1)k_l n') \\
&= k_c n' T + k_l n' \sum_{t=1}^{T-1} t \\
&= k_c n' T + k_l n' \frac{T(T-1)}{2} \\
&= k_c n + 0.5 k_l n T - 0.5 k_l n \\
(13) \quad &= \tilde{\mathcal{O}}(nT).
\end{aligned}$$

Total Replay Consider the time to train the model on n' samples is $k_c n'$. Therefore, time required to learn all the T tasks can be written as:

$$\begin{aligned}
& k_c n' + k_c(n' + n') + \dots + k_c n' T \\
&= k_c n' \sum_{t=1}^T t \\
&= k_c n' \frac{T(T+1)}{2} \\
&= 0.5 k_c n T + 0.5 k_c n \\
(14) \quad &= \tilde{\mathcal{O}}(nT)
\end{aligned}$$

PROGNN Consider the time required to train each column in PROGNN is $k_c n'$ and each lateral connection can be learned with time $k_l n'$. Therefore, time required to learn all the T tasks can be written as:

$$\begin{aligned}
& k_c n' + (k_c n' + k_l n') + \dots + (k_c n' + (T-1)k_l n') \\
&= k_c n' T + k_l n' \sum_{t=1}^{T-1} t \\
&= k_c n' T + k_l n' \frac{T(T-1)}{2} \\
&= k_c n + 0.5 k_l n T - 0.5 k_l n \\
(15) \quad &= \tilde{\mathcal{O}}(nT)
\end{aligned}$$

A.4 Simulated Results In each simulation, we constructed an environment with two tasks. For each, we sample 750 times from the first task, followed by 750 times from the second task. These 1,500 samples comprise the training data. We sample another 1,000 hold out samples to evaluate the algorithms. For SILLY-N, we have used a deep network (DN) architecture with two hidden layers each having 10 nodes. Similarly, for SILLY-N experiments we did 100 repetitions and reported the results after smoothing it using moving average with a window size of 5.

Gaussian XOR Gaussian XOR is two class classification problem with equal class priors. Conditioned on being in class 0, a sample is drawn from a mixture of two Gaussians with means $\pm [0.5, 0.5]^T$, and variances proportional to the identity matrix. Conditioned on being in class 1, a sample is drawn from a mixture of two Gaussians with means $\pm [0.5, -0.5]^T$, and variances proportional to the identity matrix. Gaussian XNOR is the same distribution as Gaussian XOR with the class labels flipped. Rotated XOR (R-XOR) rotates XOR by θ° degrees.

A.5 Real Data Extended Results FOOD1k and Mini-Imagenet datasets were obtained from <https://www.kaggle.com/datasets/whitemoon/miniimagenet> and <https://github.com/pranshu28/TAG>, respectively.

Table 3: Benchmark dataset details.

Experiment	Dataset	Training samples	Testing samples	Dimension
CIFAR 10X10	CIFAR 100	5000	10000	$3 \times 32 \times 32$
5-dataset	CIFAR-10	50000	10000	$3 \times 32 \times 32$ (resized)
	MNIST	60000	10000	
	SVHN	73257	26032	
	notMNSIT	16853	1873	
	Fashion-MNIST	60000	10000	
Split Mini-Imagenet	Mini-Imagenet	48000	12000	$3 \times 84 \times 84$
FOOD1k 50X20	Food1k	60000	99682	$3 \times 50 \times 50$ (resized)
Spoken Digit	Spoken Digit	1650	1350	28×28 (processed and resized)

Table 4: Hyperparameters for S_{ILLY}-F in spoken digit experiment.

Hyperparameters	Value
n_estimators (275 training samples per task)	10
max_depth	30
max_samples (OOB split)	0.67
min_samples_leaf	1

CIFAR 10x10 Repeated Classes We also considered the setting where each task is defined by a random sampling of 10 out of 100 classes with replacement. This environment is designed to demonstrate the effect of tasks with shared subtasks, which is a common property of real world lifelong learning tasks. Supplementary Figure 2 shows transfer of S_{ILLY}-F and S_{ILLY}-N on Task 1.

Spoken Digit experiment In this experiment, we used the **Spoken Digit** dataset provided in <https://github.com/Jakobovski/free-spoken-digit-dataset>. The dataset contains audio recordings from six different speakers with 50 recordings for each digit per speaker (3000 recordings in total). The experiment was set up with six tasks where each task contains recordings from only one speaker. For each recording, a spectrogram was extracted using Hanning windows of duration 16 ms with an overlap of 4 ms between the adjacent windows. The spectrograms were resized down to 28×28 . The extracted spectrograms from eight random recordings of ‘5’ for six speakers are shown in Figure 4. For each Monte Carlo repetition of the experiment, spectrograms extracted for each task were randomly divided into 55% train and 45% test set. The experiment is summarized in Figure 5. Note that we could not run the experiment on other 5 reference algorithms using the code provided by their authors.

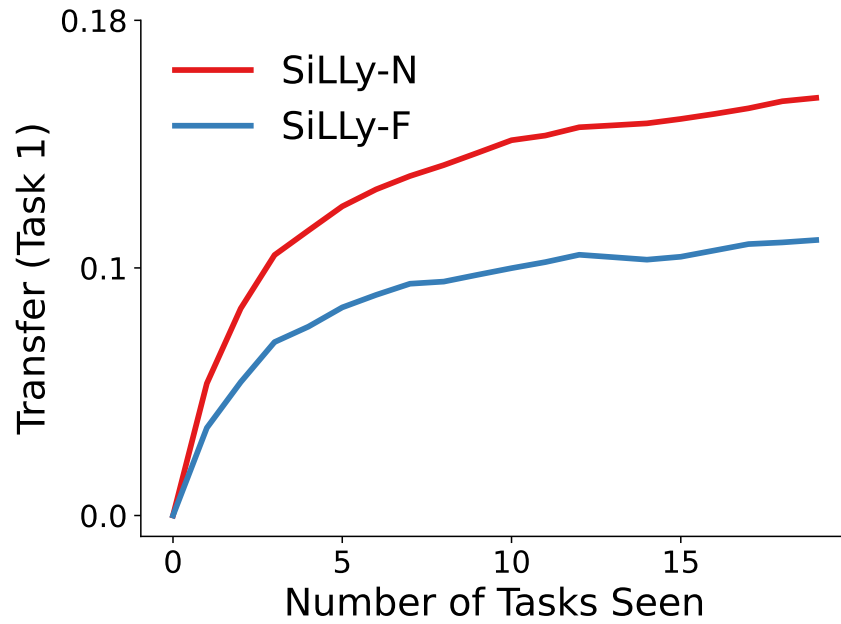


Figure 2: SiLLy-N and SiLLy-F transfer knowledge effectively when tasks share common classes. Each task is a random selection of 10 out of the 100 CIFAR-100 classes. Both SiLLy-F and SiLLy-N demonstrate monotonically increasing transfer efficiency for up to 20 tasks.

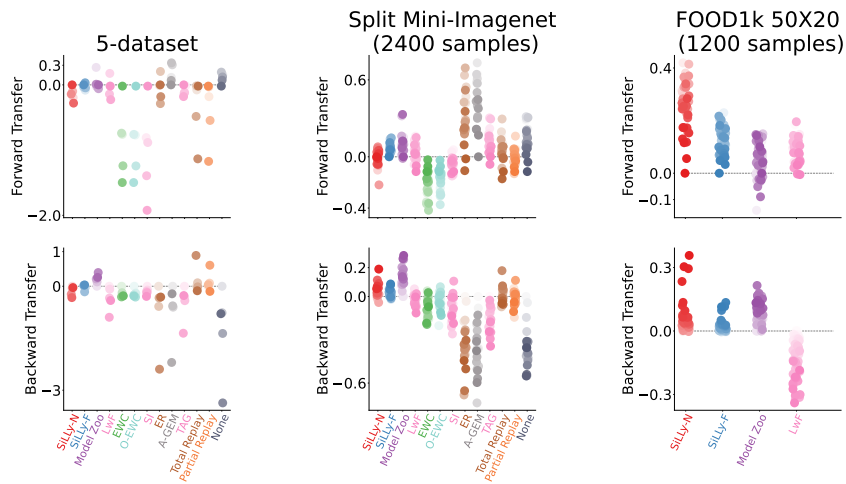


Figure 3: **Extended results on the different vision experiments.** This plot contains algorithms not shown in Figure 8.

Short-Time Fourier Transform Spectrogram of Number 5

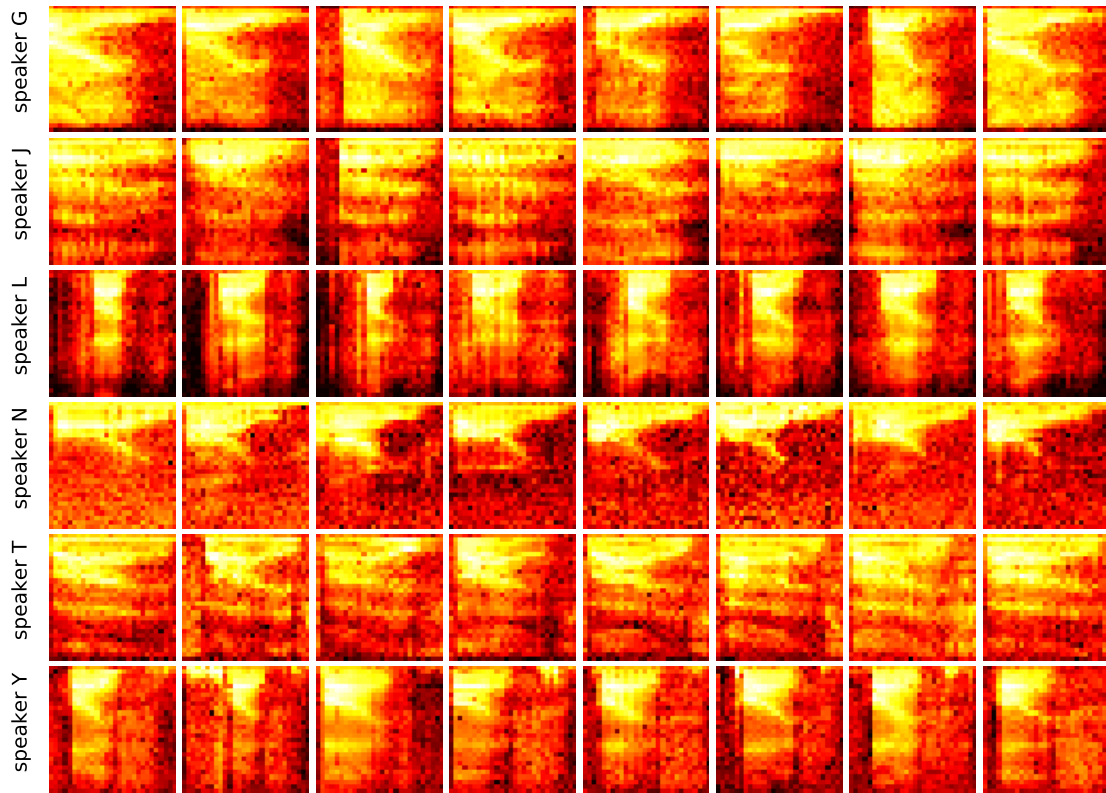


Figure 4: Spectrogram extracted from eight different recordings of six speakers uttering the digit 'five'.

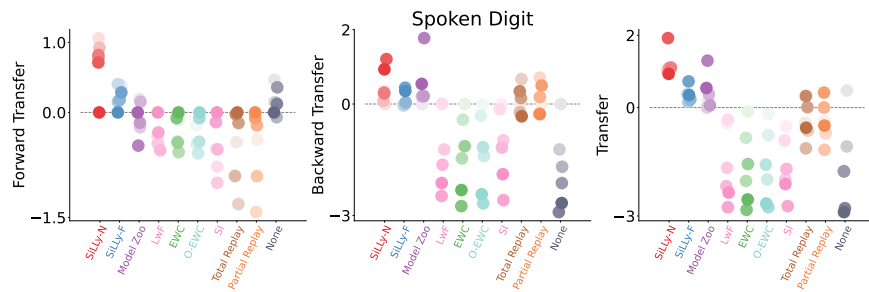


Figure 5: **Extended results on the Spoken Digit experiments.** This plot contains algorithms not shown in Figure 8.